*Journal of The Electrochemical Society*, **158** (11) H1129-H1132 (2011)
0013-4651/2011/158(11)/H1129/4/$28.00 © The Electrochemical Society



# Effect of Valence Band Offset and Surface Passivation Quality in the Silicon Heterojunction Solar Cells

**Vinh Ai Dao,[a,d] Youngseok Lee,[b] Sangho Kim,[b] Jaehyun Cho,[a] Shihyun Ahn,[a] Youngkuk Kim,[a] Nariangadu Lakshminarayan,[c,*] and Junsin Yi[a,b,z]**

[a]*School of Information and Communication Engineering, Sungkyunkwan University, Suwon, 440-746, Korea*
[b]*Department of Energy Science, Sungkyunkwan University, Suwon, 440-746, Korea*
[c]*Department of Physics, Madras Christian College, Chennai 600059, India*
[d]*Faculty of Materials Science, University of Science, Vietnam National University, Hochiminh, Vietnam*

We fabricated hydrogenated amorphous silicon/crystalline silicon (a-Si:H/c-Si) heterojunction solar cells with different intrinsic buffer layers, to elucidate the effect of the energy band gap, as well as passivation quality on the performance of the a-Si:H/c-Si heterojunction solar cells. Deformation (S-shaped) of J-V characteristics are observed in defiance of surface passivation quality for heterojunction solar cells with intrinsic buffer layers of high energy band gap ($E_g > 3.0$ eV). The deformation of J-V characteristics could be recovered when the energy band gap does not exceed 1.72 eV. In this given energy band gap, it seem to be that the surface passivation quality plays a role in heterojunction solar cell performance. The electrical-optical simulator, AFORS-HET, is used to determine the probable cause of the change in device performance. We find that the band discontinuities at the a-Si:H/c-Si interface are responsible for such an S-shaped behavior in the high energy band gap of intrinsic buffer layers.
 [DOI: 10.1149/2.031111jes] 

Manuscript submitted April 25, 2011; revised manuscript received August 1, 2011. Published October 5, 2011.

Wafer bowing and breakage caused by high-temperature metal back contact is a great concern due to the current industry trend toward thinner solar cell wafers. The hydrogenated amorphous silicon/crystalline silicon (a-Si:H/c-Si) heterojunction (HJ) solar cell is a good solution to these problems due to the low-temperature production process, around 200°C. This also limits the thermal budget and allows inexpensive, lower quality materials to be used as base material. A considerable number of studies have been made on the a-Si:H/c-Si heterojunction solar cells in recent years.[1–8] Sanyo's Heterojunction with Intrinsic Thin layer (HIT) solar cells hold the word record efficiency of 23% on a-Si:H/c-S n-type wafer, in which stacks of intrinsic buffer a-Si:H and doped a-Si:H layers help form both the emitter and the back surface field.[1] The intrinsic buffer a-Si:H (a-Si:H(i)) layer enables very high open circuit voltage, due to its excellent passivating properties. Hence, this incorporation of the a-Si:H(i) layer at the heterointerface has been confirmed to improve solar cell efficiency.[2]

The influence of band discontinuities at the a-Si:H/c-Si interface is another important issue in a-Si:H/c-Si HJ solar cells. The collection probability of photogenerated holes and also the hole (electron) piling up and hole (electron) trapping at the a-Si:H/c-Si interface are strongly dependent on the magnitude of the discontinuity in the band bending offset at the a-Si:H/c-Si interface. Reports on this value in the research literature are contradictory and range from 0.2 to 0.8 eV.[9–13] They can be classified roughly into two groups. M. Schmidt et al. suggest that an increase in the band offset is of much benefit to solar cell performance.[3] Similar results were obtained by T. H. Wang et al., who demonstrated that HJ solar cells based on n-type silicon substrate perform better than a p-type silicon substrate due to the higher band bending offset at the interface that results in lower interface recombination.[4] In contrast, Maarten W. M. van Cleef et al., supported M. Schmidt's argument in their suggestive evaluation of a-SiC:H/c-Si heterojunction solar cells. Nevertheless, they also showed that for the higher band bending offset ($\Delta E > 0.5$ eV), the deformation (S-shaped) of J-V dominated solar cell performance and when the $\Delta E < 0.3$ eV, the open circuit voltage drops with reduction in efficiency.[5] The S-shaped J-V characteristics at higher band bending offset ($\Delta E \geq 0.56$ eV) was also confirmed by A. Datta et al.[6] Eventually, in these reports the magnitude of the discontinuity in the band bending offset at the a-Si:H/c-Si interface was controlled by the energy band gap of the emitter material. In this letter, we note that the solar cell performance of the HJ cells, as influenced by the energy band gap, as well as surface passivation quality of intrinsic buffer layers had been investigated. Then, the correlation between experimental J-V characteristics and theoretical simulation indicates the probable cause of the change in solar cell performance with band offset, as well as interface defect density.

## Experimental

Figure 1 depicts the schematic structure of the fabricated solar cells. It consists of a commercial n-type Czochralski-grown (CZ) Si wafer (1-10 Ω cm, 525 μm thick, (100) oriented), cleaned sequentially using (1) acetone/methanol/DIW and (2) RCA method. Prior to intrinsic buffer layer deposition, native oxide layer was removed by 1 minute dip in 1% hydrofluoric acid. The HJ was then fabricated on the polished surface of the silicon wafer by depositing different types of intrinsic buffer layer, such as intrinsic hydrogenated amorphous silicon oxide (a-$SiO_x$:H(i)), hydrogenated amorphous silicon nitride (a-$SiN_x$:H(i)), hydrogenated amorphous silicon (a-Si:H(i)), followed by deposition of a-Si:H(p) as an emitter layer. The details of deposition process, characteristics, and optimum conditions for each type of intrinsic buffer layer can be found elsewhere.[14] ITO thin film was then deposited by RF magnetron sputtering at a substrate temperature

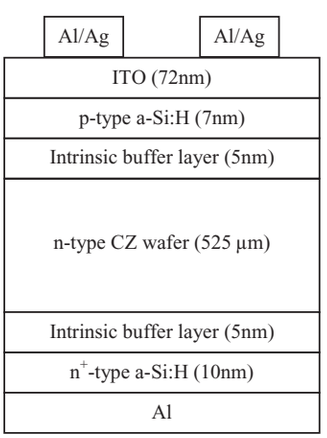


**Figure 1.** Shematic structure of Al/Ag/ITO/a-Si:H(p)/Intricsic buffer layer/c-Si(n)/Intricsic buffer layer/a-Si:H($n^+$)/Al heterojunction solar cell using in this study.

* Electrochemical Society Active Member.
z E-mail: yi@yurim.skku.ac.kr

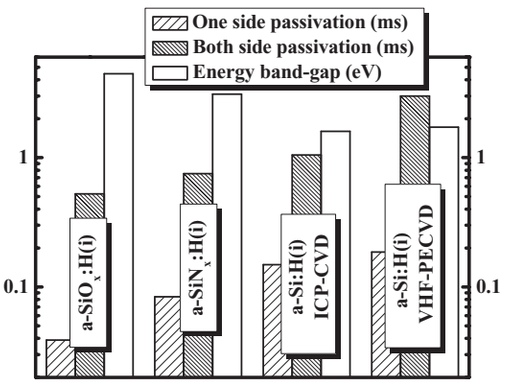


**Figure 2.** Comparison of measured minority carrier lifetime for CZ c-Si wafers passivated with different intrinsic buffer layers and energy band gap of the different intrinsic buffer layers. ICP-CVD denotes inductive couple plasma chemical vapor deposition; VHF-PECVD denotes very high frequency plasma enhance chemical vapor deposition.

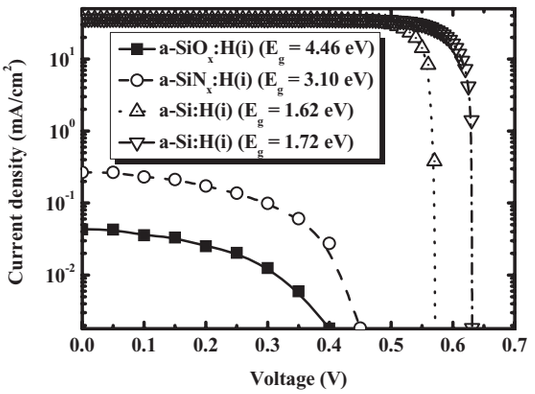


**Figure 3.** Measured J-V characteristics for the best cells with the different intrinsic buffer layers under AM 1.5 illumination.

of 200°C, followed by evaporation of a silver/aluminum finger as the emitter contacts. An $n^+$-type a-Si:H layer was deposited on the back prior to the Al back contact deposition, to create good ohmic contact. Finally, the area of the solar cell was defined by mesa etching. The active area of the solar cells was 0.36 $cm^2$.

The thickness measurements of the intrinsic buffer layers, a-Si:H(p) and a-Si:H($n^+$) films were performed using spectroscopy ellipsometry (HR-190$^{TM}$). The average value of each layer was found to be 5, 7, and 10 nm for the intrinsic buffer layers, a-Si:H(p) and a-Si:H($n^+$) films, respectively. The optical band gap was estimated from these characteristics. The minority carrier lifetime ($\tau_{eff}$) was measured by the quasi-steady-state photoconductance (QSSPC) method, using a commercial WCT-120 photoconductance set-up from Sinton Consulting to determine the quality of c-Si surface passivation. The solar cell performances was characterized by current-voltage measurements under illuminated AM1.5, 100mW/$cm^2$ conditions.

## Results and Discussion

Figure 2, the $\tau_{eff}$ is summarized, which is measured by QSSPC at an injection level of $\sim 1 \times 10^{16}$ $cm^{-3}$ on CZ-Si samples with difference type of intrinsic passivation layers, such as a-$SiO_x$:H(i), a-$SiN_x$:H(i) and a-Si:H(i). It can be observed that maximum values of the $\tau_{eff}$ with one-side passivation were 38.7, 83.9, 148.8 and 186.0 μs for a-$SiO_x$:H(i), a-$SiN_x$:H(i), a-Si:H(i) films growth by ICP-PECVD and a-Si:H(i) films deposited by VHF-PECVD, respectively. It is further revealed in Fig. 2 that the $\tau_{eff}$ with passivation on both sides of the silicon wafer showed the same trend, however, several times higher than that of a one-side passivated wafer. The $\tau_{eff}$ of the sample deposited by VHF-PECVD, which has the highest $\tau_{eff}$, exhibits more than 3 ms, one of the best values for a-Si:H(i), at 5 nm, passivated wafers. Fig. 2 illustrates the energy band gap ($E_g$) for different intrinsic passivation layers. The high $E_g$ materials, like a-$SiO_x$:H(i) and a-$SiN_x$:H(i), displayed comparatively lower values of $\tau_{eff}$ than that of a-Si:H(i) films.

Those buffer layers were used to fabricate HJ solar cells to elucidate the effect of $E_g$, as well as the $\tau_{eff}$, on performance of HIT solar cells. Fig. 3 and Table I shows the illuminated current-voltage (J-V) characteristics as well as solar cells output of the device with different intrinsic buffer layers. The S-shapes in the illuminated J-V curve were observed for the intrinsic passivation materials with high band gap. Sharp reduction was seen, not only for the open-circuit voltage ($V_{oc}$), but also for the short-circuit current density ($J_{sc}$). Hence, the device efficiency is seen to be very low, even for the excellent surface passivation of the a-$SiN_x$:H(i) with $\tau_{eff}$ of 753.3 μs. However, the deformation of the J-V curve and also device efficiency is recovered when lower band gap materials are used as intrinsic passivation layers. It is also noteworthy that the $V_{oc}$ of the device increases from 570 mV to 632 mV along with the improvement in lifetime from 1.05 ms to 3.0 ms. We achieved device efficiency of 17.43% ($V_{oc}$ = 632 mV, FF = 76.20%, and $J_{sc}$ = 36.27 mA/$cm^2$) for optimum design considerations with a-Si:H(i) (1.72 eV) acting as intrinsic passivation layer (Table I).

Fig. 4a shows J-V characteristics, concurrently, as simulated by AFORS-HET under a global solar spectrum of 1 Sun of AM1.5,[15] for various energy band gaps of the intrinsic buffer passivation layer (a-Si:H(i)). The highest performance can be observed for the lowest band gap of 1.6 eV. These seem to be a slight reduction in device performance for further increase in $E_g$, up to a value of 1.72 eV. However, this reduction is negligible, as shown by numerical values in Table II. Deformation in the J-V curve begins to develop with an energy band gap beyond 1.72 eV. As shown in Fig. 4b, the band energy diagram for the simulated structure with different energy band gaps is simulated to identify the cause of the distortion in the illuminated J-V curve with the high energy band gap. There is no variation in the valence band offset ($\Delta E_v$) when the energy band gap of intrinsic buffer layers increases from 1.62 eV to 1.72 eV (Table II). However, further increase in the energy band gap results in the increase of $\Delta E_v$ (Table II). It is noteworthy that the variation of device performance and the $\Delta E_v$ are in opposing directions. The hole accumulation at the a-Si:H/c-Si interface is enhanced with increasing $\Delta E_v$,[6] and thus a fall in FF for $\Delta E_v \geq 0.55$ eV. These results are in good agreement with van Cleef et al. and Rahmouni et al.[5,16] They demonstrate that

**Table I. Photovoltaic parameters of HIT solar cells fabricated with different intrinsic buffer layers.**

| Intrinsic buffer layers | $E_g$ (eV) | $\tau_{eff}$ (ms) | $J_{sc}$ (mA/$cm^2$) | $V_{oc}$ (mV) | FF | η (%) |
|---|---|---|---|---|---|---|
| a-Si:H(i) | 1.62 | 1.050 | 36.3 | 570 | 76.00 | 15.73 |
| a-Si:H(i) | 1.72 | 3.000 | 36.27 | 632 | 76.20 | 17.43 |
| a-$SiN_x$:H(i) | 3.10 | 0.753 | 0.267 | 450 | 28.71 | 0.034 |
| a-SiOx:H(i) | 4.46 | 0.525 | 0.043 | 450 | 29.58 | 0.005 |

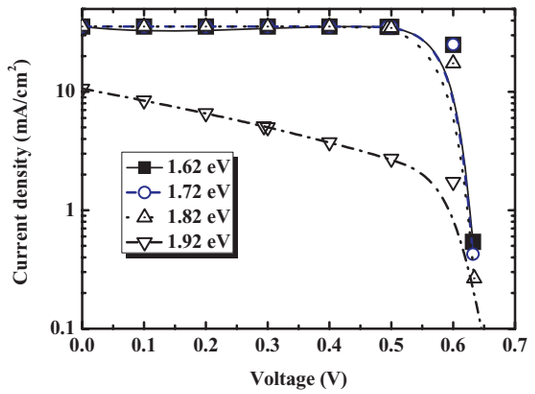


(a)

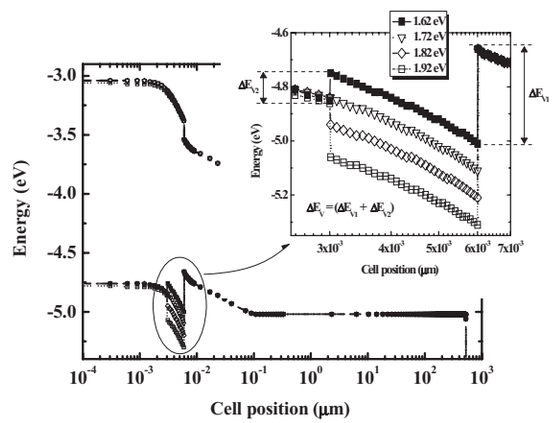


(b)

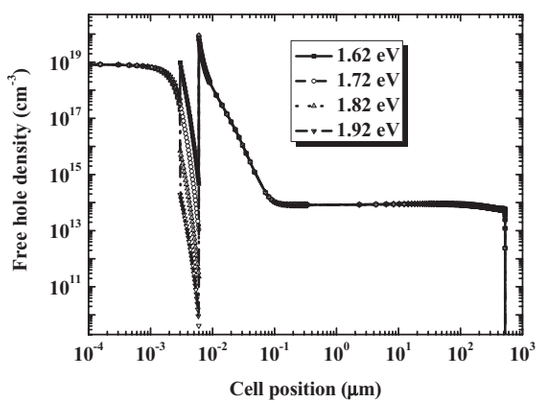


(c)

**Figure 4.** (a) Simulated illuminated J-V characteristics, (b) the band diagram under AM 1.5 light, (c) the free hole density under the same conditions, as a function of position in the device for different values of energy band gap of intrinsic buffer layers.

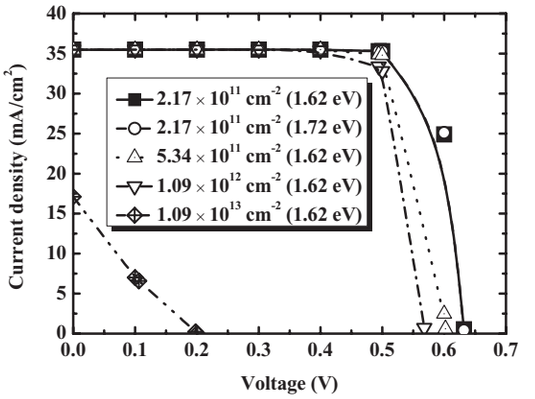


(a)

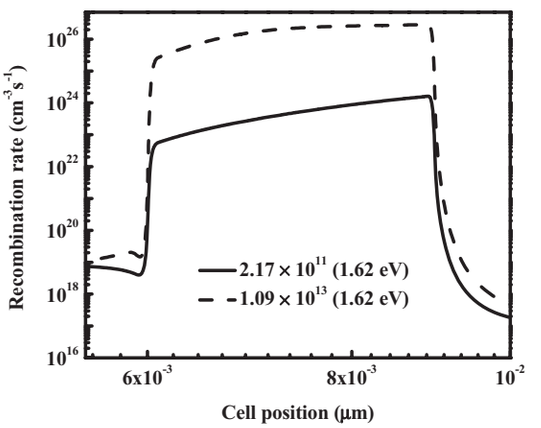


(b)

**Figure 5.** (a) Simulated illuminated characteristics and (b) simulated recombination rate under AM1.5 light, as a function of position in the device for different values of the density of interface defects.

with $\Delta E_v \geq 0.56$ eV, by changing the band gap of emitter layers, the S-shaped characteristics begin to develop. In our case, from Fig. 4c, when $\Delta E_v \geq 0.55$ eV, free holes accumulate at the entire interface and also get trapped in the interface states at the back of the a-Si:H(i) layer. This leads to a reduction in the electric field and flat bands over the depletion region at the interface, Fig. 4b. This results in a fall in the FF and conversion efficiency as shown in Table II. There is an abrupt fall not only of the FF but also the $J_{sc}$, especially for the $\Delta E_v = 0.64$ eV. In this case, photogenerated holes coming from the crystalline n-type side have difficulties in reaching the emitter layers due to the potential barrier in the valence band. This could lead to a strong pile up of holes at the interface, resulting in a deep depletion at the interface (Fig. 4b). Hence, the hole current is nearly suppressed, eventually resulting in a lower current and also low fill factor.

Table I and II shows the experimental and simulation results for HIT solar cells, as a function of the energy band gap of intrinsic passivation layers, as well as the density of interface defects (or minority carrier lifetime) at the hetero-interface. By simulation, in which the interface density was fixed at $2.17 \times 10^{11}$ (cm$^{-2}$), the results indicate that the device performance is almost the same with increasing energy band gap from 1.62 eV to 1.72 eV (Table II). However, this was contrary to the device behavior observed in the experiment (Table I). The discrepancies between the simulation and experimental result are attributed to a reduction of measured minority carrier lifetime from 3 ms to 1.05 ms, resulting from a high defect density at the interface, which in turn, leads to a reduction of $V_{oc}$ from 632 mV to 570 mV, as seen from the experimental results (Table I). The device performance as a function of defect density at the interface, concurrently, is modeled in order to explain the difference berween the simulation and experimental results.

Fig. 5a and Table II show the J-V curve and numerical values of parameters for the device simulated under AM1.5 light, as a function of the density of interface defect ($D_{it}$). Apparently, from the figure, the highest $V_{oc}$ appears for the HIT cell with interface defect states of $2.17 \times 10^{11}$ cm$^{-2}$; there is progressive reduction in $V_{oc}$ with increasing density of interface defects. The deformed J-V curves were observed

**Table II. Photovoltaic parameters of HIT solar cells simulated with different intrinsic buffer layers band gap, as well as density of interface defects.**

| $E_g$ (eV) | $\Delta E_V$ (eV) | $D_{it}$ ($cm^{-2}$) | $J_{sc}$ ($mA/cm^2$) | $V_{oc}$ (mV) | FF | η (%) |
|---|---|---|---|---|---|---|
| 1.62 | 0.45 | $2.17 \times 10^{11}$ | 35.5 | 632 | 77.72 | 17.44 |
| 1.62 | 0.45 | $5.34 \times 10^{11}$ | 35.5 | 610.2 | 79.9 | 17.32 |
| 1.62 | 0.45 | $1.09 \times 10^{12}$ | 35.49 | 568 | 81.7 | 16.47 |
| 1.62 | 0.45 | $2.17 \times 10^{12}$ | 35.5 | 494.5 | 77.84 | 13.66 |
| 1.62 | 0.45 | $1.09 \times 10^{13}$ | 17.07 | 197.7 | 20.74 | 0.7 |
| 1.72 | 0.45 | $2.17 \times 10^{11}$ | 35.48 | 632 | 77.72 | 17.43 |
| 1.82 | 0.55 | $2.17 \times 10^{11}$ | 35.49 | 633.6 | 76.28 | 17.15 |
| 1.92 | 0.64 | $2.17 \times 10^{11}$ | 10.57 | 660.2 | 21.52 | 1.502 |

when the density of the interface defect is beyond $1.09 \times 10^{12}$ ($cm^{-2}$). As reported by *Jensen* et al., the $V_{oc}$ value of the HJ solar cells is limited by interface recombination as described earlier.[17]

$$V_{oc} = \frac{1}{q}\left\{\phi_c - AkT \ln\left(\frac{qN_vS_{it}}{j_{sc}}\right)\right\} \quad [1]$$

where $S_{it}$ is the interface recombination velocity, $\phi_c$is the effective barrier height in c-Si, $N_v$ is the effective density of states in the valence band, $kT$ is the thermal energy, $A$ is the diode ideality factor, $j_{sc}$ is the short circuit current density, and $q$ denotes the elementary charge. We can deduce from Eq. 1 that a lower density of interface defects results in lower $S_{it}$ and hence an increased $V_{oc}$. Moreover, the results indicate that the density of interface defects is required to be less than $5.34 \times 10^{11}$ $cm^{-2}$ to obtain good performance, as is seen from earlier research literature.[8] Particularly, for an interface density $\geq 1.09 \times 10^{13}$ $cm^{-2}$, a large number of holes get trapped at the a-Si:H/c-Si interface, results in accumulation of holes in these states.[6] This can be the reason for reducing of the number of holes comming and attracting of electrons at this interface, resulting in the faster recombination with increased density of interface defects [Fig. 5b], hence lower the power generation, in terms of lower in current density as well as fill factor (Table II and Fig. 5a).

Eventually, from both the numerical analysis and experiment results, we can conclude that either the high energy band gap of the intrinsic passivated layer or the high density of interface defects at the interface is the probable cause of such an S-shape illuminated I-V. We can interpret the curve of Figs. 2 and 3 by defining two regimes, namely the high and low band gap regimes. In the first regime, a high value of band gap (a-$SiO_x$:H(i), a-$SiN_x$:H(i)), results in high valence band offset, lower electron affinity and opposes the flow of the photo current in the device. Hence, the valence band bending offset is a dominant parameter. Conversely, in the second regime where the energy band gap is $\leq$1.72 eV, an investigation of both the energy band gap and measured lifetime showed a decrease in device performance with lowering of the energy band gap. The simultaneous highest measured lifetime and highest device performance with a-Si:H(i) deposited by VHF-PECVD indicates that surface passivation at the interface plays an important role in performance of heterojunction with intrinsic thin layer solar cells.

## Conclusions

We studied the performance of HIT solar cells on n-type CZ-silicon substrates with the changing of the energy band gap, as well minority carrier lifetime, using both experimental studies and computer simulation. The obtained results revealed the appearance of an S-shaped J-V curve, when a high energy band gap material ($E_{g>}$ 3.0 eV) is used as an intrinsic buffer layer. This could be attributed to accumulation of holes at the interface that results in surface recombination, and in turn to reduced cell performance. The S-shaped J-V disappeared at a reduced energy band gap value $\leq$1.72 eV. In this energy band gap region, device performance depends on surface passivation quality. The high measured minority carrier lifetime at the interface results in high $V_{oc}$, as well as FF, and hence better solar cell efficiency. The photovoltaic parameters of an optimum design device were found to be $V_{oc}$ = 631 mV, $J_{sc}$ = 36.27 $mA/cm^2$, fill factor = 76.20% and efficiency = 17.43%

## Acknowledgment

This research was supported by the WCU (World Class University) program through the National Research Foundation of Korea funded by the Ministry of Education, Science and Technology (R31-2008-000-10029-0).

## References

1. T. Mishima, M. Taguchi, H. Sakata, and E. Maruyama, *Solar Energy Materials & Solar Cells* **95**, 18 (2011).
2. M. Taguchi, K. Kawamoto, S. Tsuge, T. Baba, H. Sakata, M. Morizane, K. Uchihashi, N. Nakamura, S. Kiyama and O. Oota, *Prog. Photovoltaics: Research and Applications*, 503 (2000).
3. M. Schmidt, L. Korte, A. Laades, R. Stangl, Ch. Schubert, H. Angermann, E. Conrad, K. v. Maydell, *Thin Solid Films* **515**, 7475 (2007).
4. T. H. Wang, M. R. Page, E. Iwaniczko, D. H. Levi, Y. Yan, H. M. Branz, and Q. Wang, *the 14th Workshop on Crystalline Silicon Solar Cells and Modules, American*, August 2004.
5. M. W. M. van CLEEF, F. A. Rubinelli, R. Rizzoli, R. Pinghini, R. E. I. Schropp, and W. F. van der WEG, *Jpn. J. Appl. Phys.* **37**, 3926 (1998).
6. A. Datta, M. Rahmouni, M. Nath, R. Boubekri, P. Roca I Cobarrocas, P. Chatterjee, *Solar Energy Material & Solar Cells* **94**, 1457 (2010).
7. V. A. Dao, Y. S. Lee, S. H. Kim, Y. K. Kim, N. Lakshminarayan, and J. Yi, *Journal of The Electrochemical Society* **158**, 312 (2011).
8. L. Korte, E. Conrad, H. Angermann, R. Stangl, M. Schmidt, *Solar Energy Material & Solar Cells* **93**, 905 (2009).
9. J. Essick and Z. Nobel, Y. M. Li, M. S. Bennett, *Phys. Rev. B* **54**, 4885 (1996).
10. R. Fang and L. Ley, *Phys. Rev. B* **40**, 3818 (1989).
11. F. Evangelisti, *J. Non-Cryst. Solids* **77/78**, 969 (1985).
12. M. Mahmudur Rahman and S. Furukawa, *Jpn. J. Appl. Phys.* **23**, 515 (1984).
13. L. Magafas, N. Georgoulas and A. Thainailakis, *Semicond. Sci. Technol.* **7**, 1363 (1992).
14. V. A. Dao, Ph. D. Thesis, School of Information and Communication Engineering, Sungkyungkwan University, Suwon, 2011.
15. R. Stangl, J. Haschke, C. Leendertz, published in the InTech e-book: "SolarEnergy", ISBN 978-953-7619-X-X, Dez 2009.
16. M. Rahmouni, A. Datta, P. Chatterjee, J. Damoon-Lacoste, C. Ballif, P. Roca i Cabarrocas, *J. Appl. Phys.* **107**, 054521 (2010).
17. N. Jensen, R. M. Hausner, R. B. Bergmann, J. H. Werner, U. Rau, *Progress in Photovoltaics: Research and Applications*, 2002, pp 1-13.